QUANTITATIVE PRECIPITATION ESTIMATION BY X-BAND POLARIMETRIC RADAR NETWORK OF KOCHI UNIVERSITY

Akira Nishii[1] and Koji Sassa[2]

[1]*Graduate school of Kochi University, 2-5-1, 780-8072 Akebono-cho, Kochi-shi, Kochi, Japan*
[2]*Kochi University, Kochi, 2-5-1, 780-8072 Akebono-cho, Kochi-shi, Kochi, Japan*

(Dated: 2 July 2018)

1 Introduction

Kochi prefecture locates in the south part of Shikoku Island divided by Shikoku mountains of more than 1500 m in height, and it also faces warm and moist Pacific Ocean. Then, this area is one of the heaviest rainfall area in Japan. Annual precipitation amounts in Kochi city and in mountain area are about 2,500 mm and more than 3000 mm, respectively. Heavy rain events of more than 50 mm/h occur frequently. Many heavy rain events are affected by complex terrain of Kochi Prefecture. Warm rain events are also frequently observed. Moreover, tornadoes often occur. Japan Meteorological Agency (JMA) provides the 2km CAPPI data obtained from its C-band radar network every 5miniutes. We often miss cumulonimbi developing rapidly and approaching tornadoes. As another monitoring system, Ministry of Land, Infrastructure and Transport (MLIT) has constructed X- and/or C- band polarimetric radar network called XRAIN providing the data every 1 minute. However, only a C-band polarimetric radar located in a high mountain (1500 m above sea level) covers Kochi prefecture and there is no X-band polarimetric radar covering this area. Therefore, we have been constructing our own X-band polarimetric radar network to complement the other radar networks in Kochi prefecture. At this time, we have installed 5 X-band polarimetric radars and one more radar will be installed in October 2018. We have also developed quasi-real time Quantitative Precipitation Estimation (QPE) system providing 1km CAPPI data of 150 m in spatial resolution every 1 minute from our radar network. QPE by X-band polarimetric radar have achieved very high performance in many studies (e.g., Maki et al., 2005). Especially QPE with specific differential phase K_{DP} achieves high performance because K_{DP} is less sensible of the variation of Drop Size Distribution (DSD) and can compensate attenuation by rainfall (Park, et al., 2005). The present study aims to verify our QPE system. We evaluated of QPE from three radars at Asakura, Monobe, and Aki radar sights. We also introduce our polarimetric radar network system.

2 Kochi University Polarimetric Radar Network

Figure 1 shows the arrangement of Kochi University X-band polarimetric radar network. 5 radars have currently installed and they cover the most part of Kochi prefecture. Asakura, Monobe, Aki radars shown in green circles have been operated for more than three years. In this year, we installed Susaki and Tosashimizu radars shown by yellow circles in western Kochi. Kuroshio radar shown by red circle will be settled in October 2018. The observation range of Asakura radar is 80 km and those of the other radars are 30km. In the present study, we evaluated QPE for three radars; Asakura, Monobe and Aki because they have a lot of data for more than two years. The specifications of these radars are listed in table 1. Our radars are relatively

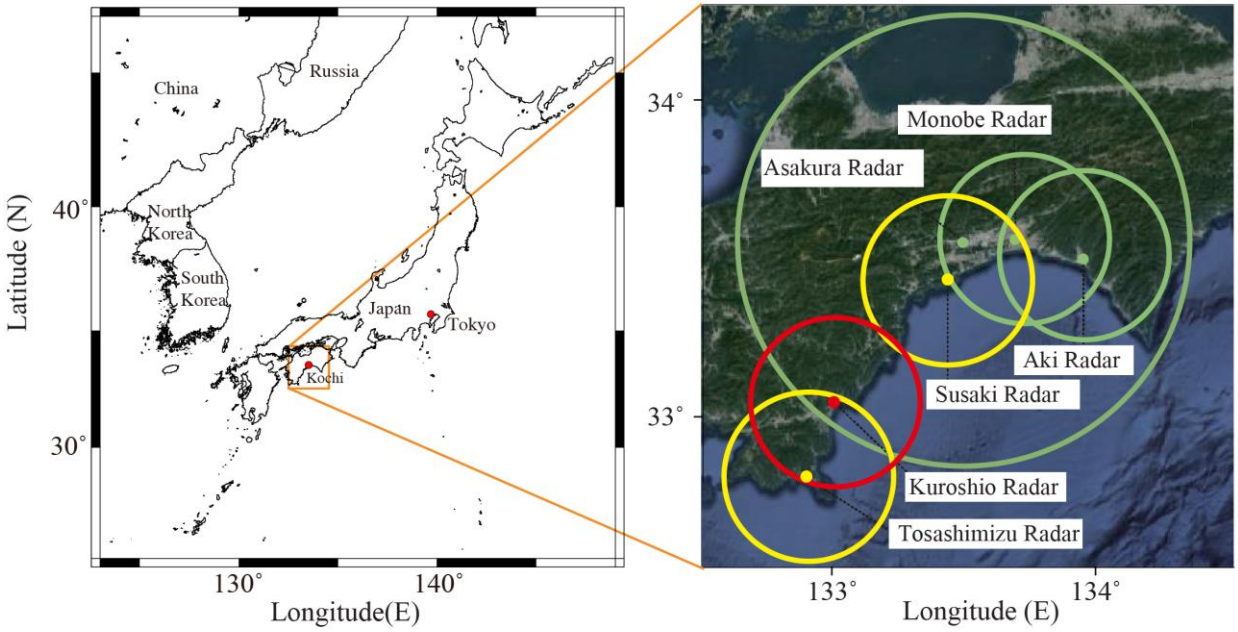

Figure 1:The location of Kochi and Kochi University radar network.
Points and circles represent radar locations and observation ranges, respectively.

Table 1: System specifications of Kochi University's radars.

	Asakura	Monobe, Aki
Frequency	9.39 GHz	9.47 GHz
Beam width	2.0 deg	2.7 deg.
Range resolution	150 m	50 m
Observation range	80 km	30 km
Update time	1 min (low elev.) 5 min (high elev.)	1 min

cheap and compact then the beam widths are slightly wide. But, range resolutions are high. At this time, we operate Asakura radar in the volume scan mode composed of 3 PPI scans of 2.5, 4.0 and 6.0 deg. in elevation angle every 1 minute and 5 PPI scans at higher angles up to 20 deg. every 5 minutes though the elevation angles employed for the validation of QPE were slightly different as mentioned later. Monobe and Aki radars are operated in 5 PPI scans from 3.0 deg. to 16 deg. every 1 minutes. These observation data are immediately transferred to science cloud at National Institute of Information and Communications Technology (NICT) and converted into rainfall intensity R [mm/h]. R is provided as 1km CAPPI data with of 150 m × 150 m in spatial resolution. It takes less than one minute from the volume scan of each radar to make radar network data. We adopted lower altitude for CAPPI data than those provided by JMA or XRAIN (2 km altitude) because we wanted to observe the altitude near the surface as well as possible in complex terrain of Kochi prefecture and expected to observe warm rain which developed at lower altitude. To make CAPPI from PPI data observed by each radar, we employed Cressman interpolation method (Cressman, 1959). The sampling radius of the interpolation are defined as follows;

For Asakura radar (r is a distance from radar [km]);

Horizontal sampling radius [km]: $0.01r + 0.1$ *(2.1)*

Vertical sampling radius [km]: 0.75 (constant.) *(2.2)*

For other radars;

Horizontal sampling radius [km]: $0.02r + 0.2$ *(2.3)*

Vertical sampling radius [km]: 2.5 (constant.) *(2.4)*

The difference in sampling radius is based on the observation range and the adopted PPI elevations for CAPPI. Figure 2 shows the example of CAPPI data of our radar network. We employed the highest value of precipitation intensity among each radar data in the area where more than two radars cover in order to compensate rain attenuation.

3 Quality Control of Our Radar Network

Our radars are settled at relatively lower altitude in complex terrain area. Therefore, our radars are strongly affected by clutters and beam blockage by mountains. Moving Target Indicator (MTI) is applied in our radars to remove contamination by clutters (Aoyagi, 1983). However, it is not enough to remove clutters and many echoes remain even in sunny days as shown in the upper figures of Fig. 3. Then we made additional processing to remove clutters. For Asakura radar, both the original received power Pr and the MTI-processed power $Pr_{\_MTI}$ are available. The reflectivity data are employed when the difference between $Pr_{\_MTI}$ and Pr is more than 5 dBZ as shown in following inequality,

$$Pr_{\_MTI} - Pr \geq 5\ dBZ. \qquad (3.1)$$

Otherwise, the data were eliminated as clutters. Monobe and Aki radars do not output original Pr and do only MTI-processed radar reflectively Z. Therefore, we removed clutters by mapping. We checked strong reflectivity Z areas in sunny days affected by clutters and removed them. Results of these elimination processes are shown in the lower figures of Fig. 3. Most of clutters are dramatically removed by these processes. Terrains also become as partial blockages of radar beam. In far side of such terrains, Z becomes lower even heavy rainfall and QPE is underestimated. To avoid such situation, we masked partial beam blocked area. Figure 4 shows the examples of masked areas. We employed the PPI data obtained at higher elevation angles to interpolate Z and K_{DP} eliminated as clutters. Moreover, the data in the region where ρ_{hv} was less than 0.60 were eliminated to remove echo returning from a non-meteorological target. We also made the attenuation correction with the method of Maesaka et al.(2014) to correct rain attenuation.

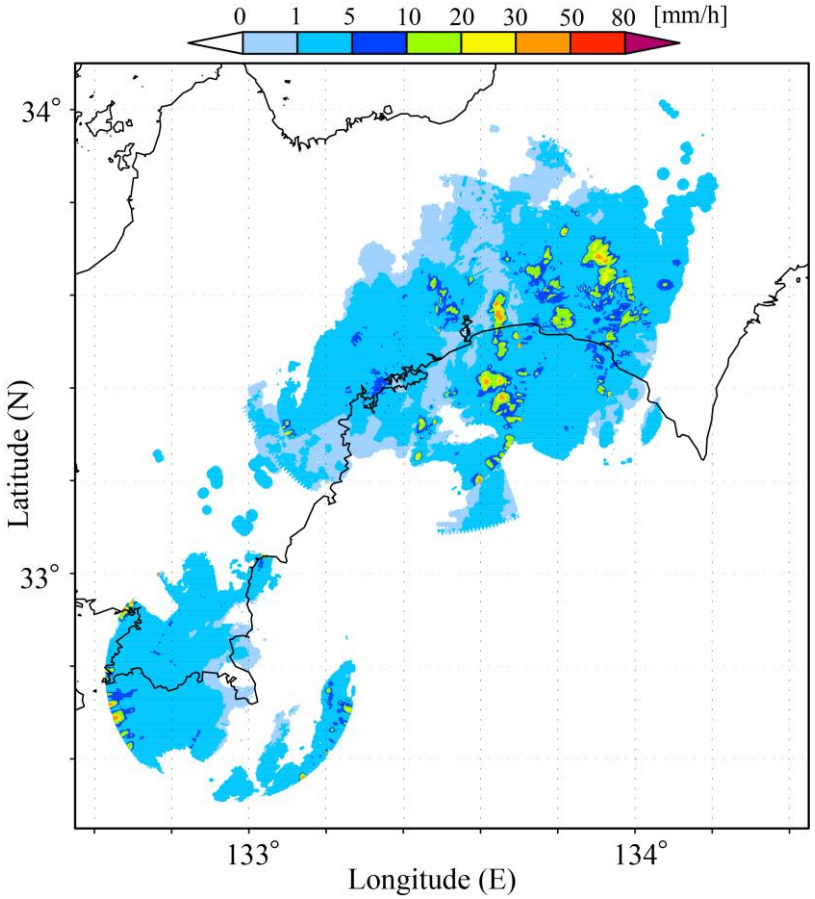

Figure 2: A picture of rainfall intensity derived from the radar network. This shows CAPPI at a height of 1 km. (At 09:06 UTC, May 13, 2018)

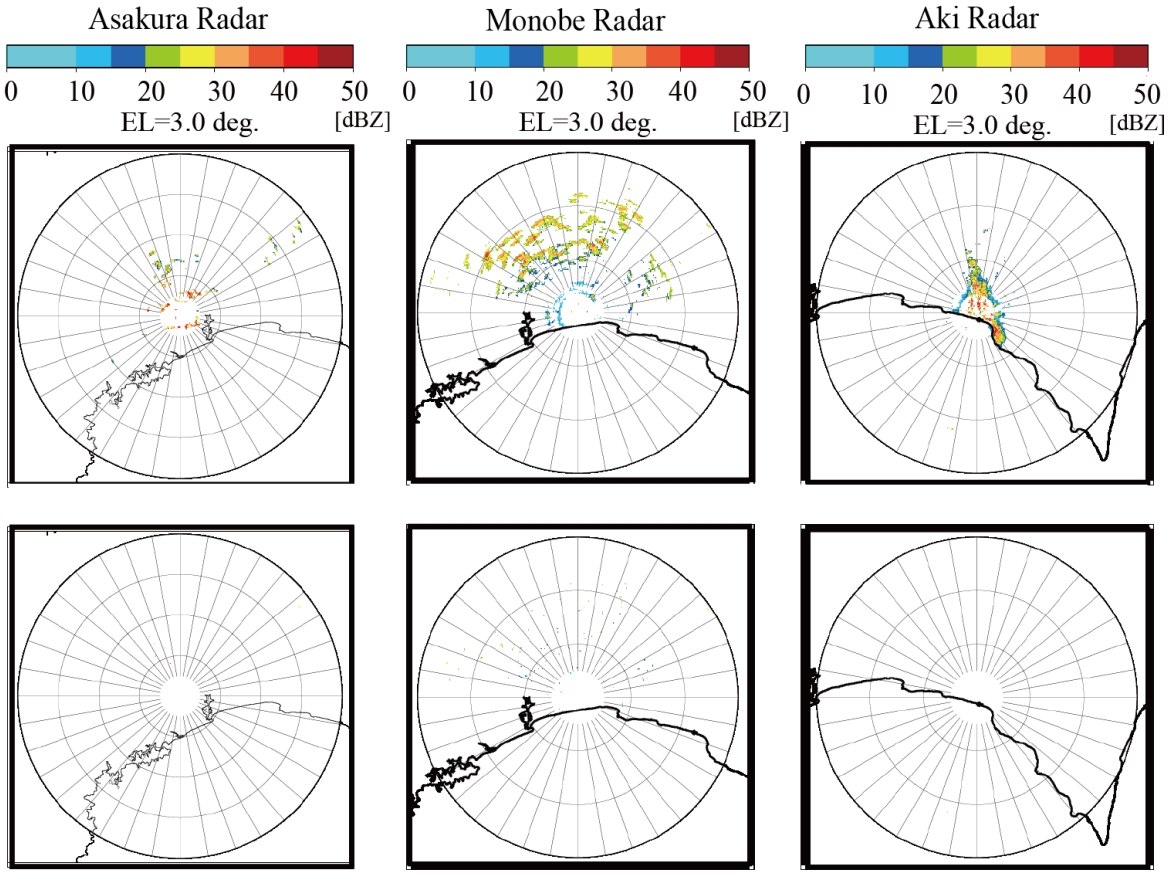

Figure 3 PPI images of reflectivity before (a) and after (b) removing clutter by our methods.

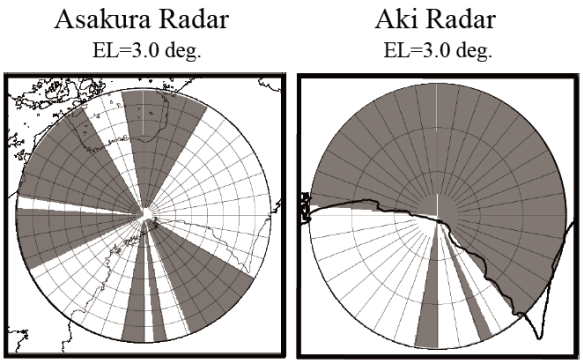

Figure 4 Examples of masked area shown in gray shade.

4 QPE by radars

We employed specific differential phase K_{DP} [deg./km] and horizontal radar reflectively Z [mm^6/m^3] in QPE. We converted these parameters to rainfall intensity R [mm/h] by the following equations,

$$K_{DP} = \alpha \times 19.6 K_{DP}^{0.825} \ (Z \geq 30 \text{ dBZ and } K_{DP} \geq 0.3), \quad (4.1)$$

$$Z = BZ^{\beta}. \quad (4.2)$$

K_{DP}–R relationship (eq. 4,1) is based on Maki et al. (2005)'s equation derived from DSD observation in Tsukuba, Japan. But we found that this relationship underestimates rainfall intensity. Therefore, we introduced the correction coefficient, α=1.3. Such underestimation also occurs in XRAIN which uses the same α (Maesaka et al., 2014). K_{DP} is a good parameter for QPE because of its less sensitivity to DSD variation than Z and resistance to attenuation by rain (Park et al., 2005). But in weak rainfall, the value of K_{DP} is quite low and noise contamination is not negligible. Therefore, Z-R relationship was adopted for weak rain. The values of constant B and β in Z-R relationship (eq. 4,2) are decided for each radar by comparing between hourly rainfall observed by rain gauges and the integrated value of instantaneous Z for one hour as mentioned later.

5 Verification of QPE

To evaluate the accuracy of QPE defined in chapter 4, we compared radar rainfall R_r [mm] and gauge rainfall R_g [mm]. We picked up 4 heavy rainfall events (max hourly rainfall was more than 20 mm/h.) as shown in Table 2.

Table 2 Periods of events.
Note that date is in UTC and all event occurred in 2017.

Rainfall period
09:00 May 12 – 0:00 May 13
08:00 June 20 – 23:00 June 20
01:00 August 6 – 07:00 August 7
14:00 September 16 – 14:00 September 17

We used the PPI scan data of 3, 4, and 5 deg. in elevation angle for Asakura radar in order to validate QPE. The elevation angles slightly different from the current observation mode. For the validation of Monobe radar and Aki radar, we used 5 PPI scan data from 3 deg. to 16 deg. We also used 10 minutes rainfall intensity obtained from 30 rain gauges of JMA AMeDAS and POTEKA installed by us as shown in Fig. 5, in order to compare with rainfall intensity obtained by our radars. All rain gauges were tipping bucket type and minimum resolution is 0.5 mm. We compared with the radar data at 1 km height because we provided the CAPPI data at that height. But radar beam does not reach at some rain gauge sites because it is blocked by terrain. In such case we employed the data obtained from the PPI scan higher elevation angles but close to 1 km height.

Even after quality control, the observation error and the radio wave dissipation sometimes occur. Thus we removed the data in the following situations,

- R_g and/or R_r was 0 mm.
- There was at least 1 missing data in R_r.

6 Result of verification

Results of validation of *Z-R* relations are shown in Figure 6. We employed stratified average per 1 dBZ radar reflectivity from 20 dBZ to 30 dBZ for Z to calculate *B* and *β*. In addition to *Z-R* relationship variability for radar calibration, it is also largely affected by the variation of DSD and coefficients differs each rainfall type (e.g. Fujiwara (1965). It is impossible to

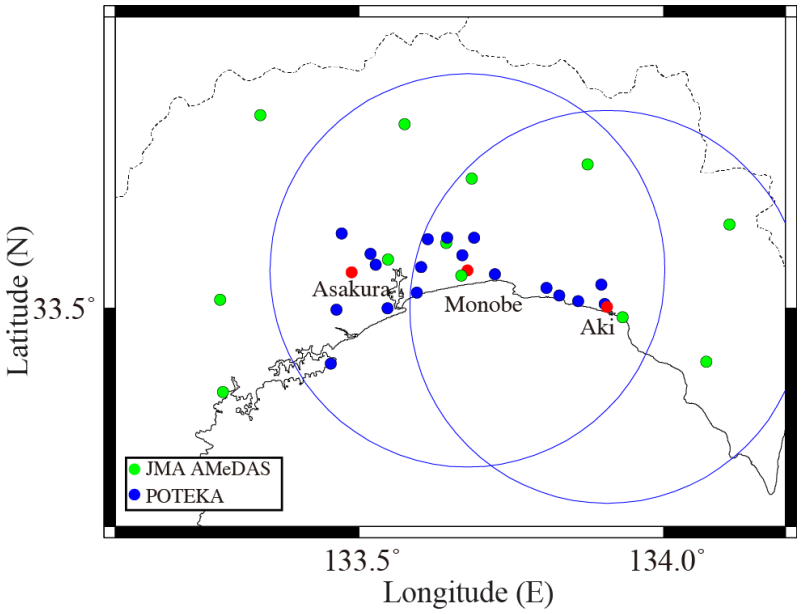

Figure 5 Map of rain gauges. Green dots and Blue dots denote the locations of JMA AMeDAS rain gauge and POTEKA rain gauge, respectively. Red points denote radar sites and blue circles represent the observation ranges of Monobe radar and Aki radar.

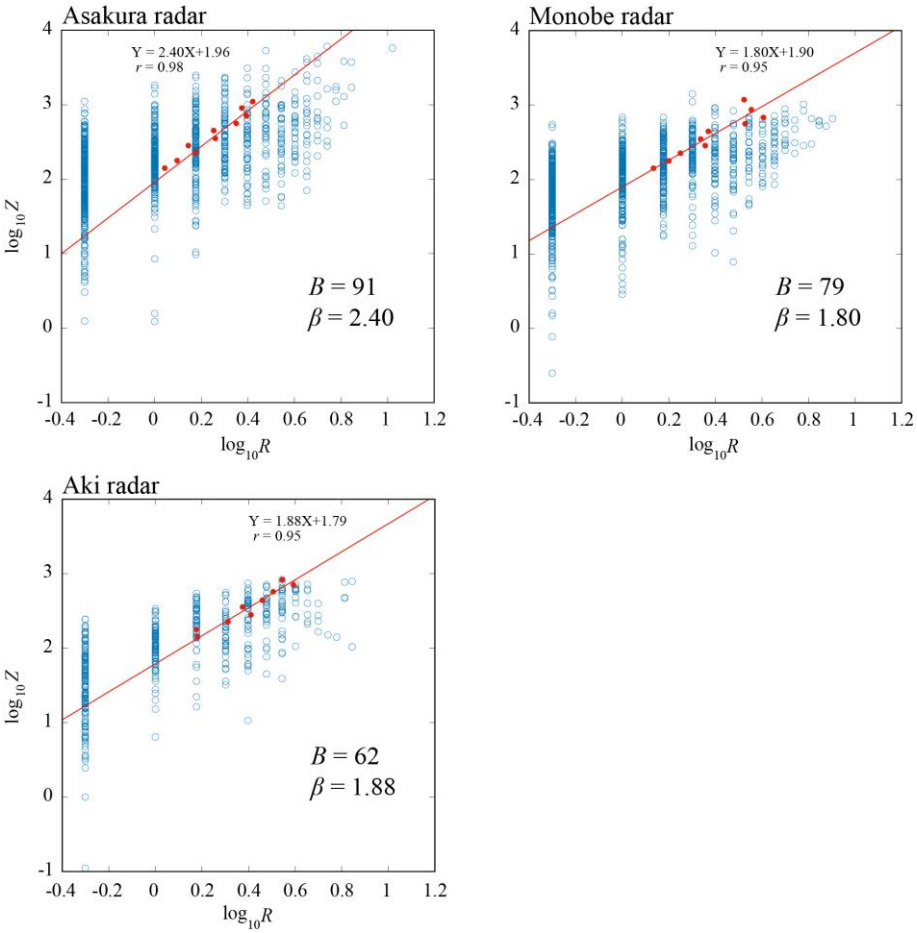

Figure 6 Logarithmic plots of Z-R relationship.
Red points show layer averages to calculate Z-R relationships and red lines shows regression line.

adopt *Z-R* relationship for each rain event, thus we employed unique coefficients for each radar.

Figure 7 shows the result of verification of total QPE. Asakura radar and Aki radar were found to slightly underestimate rainfall however correlation coefficients achieved about 0.80. each radar estimated rainfall almost accurately. For heavy rain case, K_{DP}-*R* relationship shown by green plots mainly contributes to QPE. We found that QPE with K_{DP}-*R* relationship showed high performance. The reason of underestimate is due to radio wave dissipation blocked by complex terrain. Especially, Aki radar locates near mountains. The PPI data at higher elevation angle to interpolate such masked region may not represent the actual clouds well. Asakura radar is also affected by complex terrain. On the other hand, Monobe radar locates at open plain field and not affected by clutters. Therefore, Monobe radar showed good performance, i.e., a = 1.01 and r = 0.79.

Figure 8 shows the result of a typical irregular observation point. The rain gauge at Kochi city hall located 3.8 km from Asakrua radar. In this case, Asakura radar strongly over-estimated the rainfall intensity. This rain gauge is also covered by Monobe radar but it did not show the abnormal data. Therefore, such results were not caused by the error of the rain gauge. Figure 9 shows the range dependence of differential phase φ_{DP} at the azimuth of 72 deg. which showed the direction of Kochi city hall. There is a peak of φ_{DP} near 5 km from Asakura radar. It is abnormal value because φ_{DP} should increase monotonically below a melting layer. It is not caused by switching between short and long pulses because the change from short pulse to long pulse is made at 10km from Asakura radar. In this study, we applied smoothing filter twice to smooth the fluctuation of φ_{DP}. Hubbert and Bringi (1995) used moving average filter for 10 times to remove φ_{DP} noises. But, the jump of φ_{DP} at 5 km will not be smoothed by filters. This may be caused by the ghost echo due to clutter in far distance, power cable crossing between Asakura radar and Kochi city hall and so on. The investigation of the reason is one of our future work.

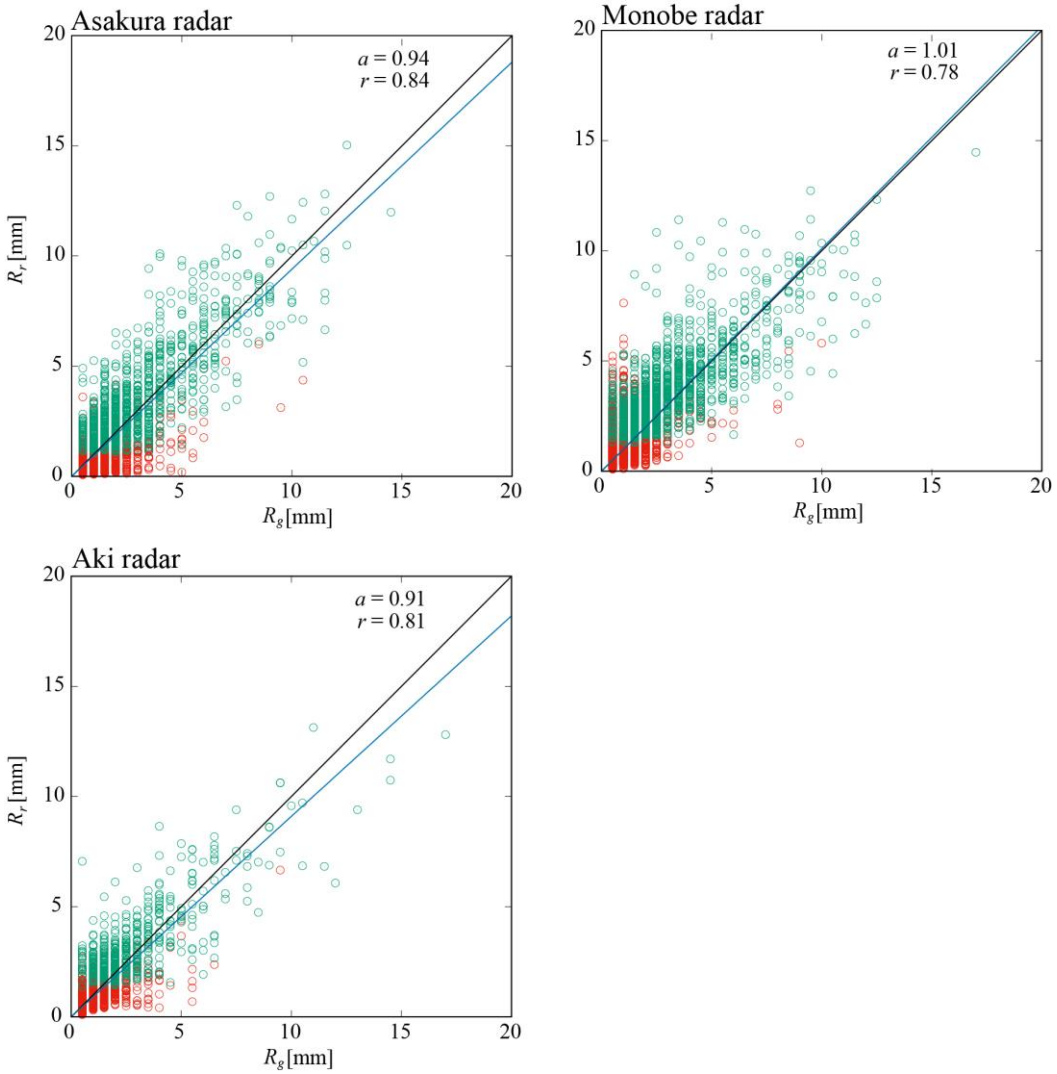

Figure 5 Scatter plots of Rr and Rg for each radar. Blue line and black line represent Rr=Rg and Regression line, respectively. Green plots indicate Rr estimated with K_{DP}-R relationship more than 50 % in estimated time and Red plots show Rr with Z-R relationship.

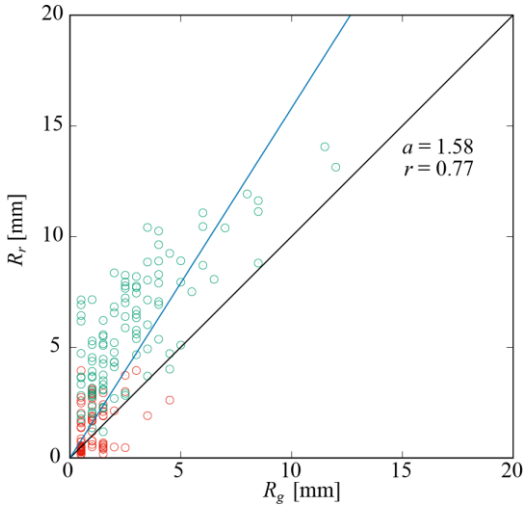

Figure 6 Scatter plots of Rr derived from Asakura radar and Rg at Kochi city hall. Blue line and black line represent Rr=Rg, Regression line, respectively. Green plots indicate Rr is estimated with K_{DP}-R relationship equal or more than 50 % in estimating time.

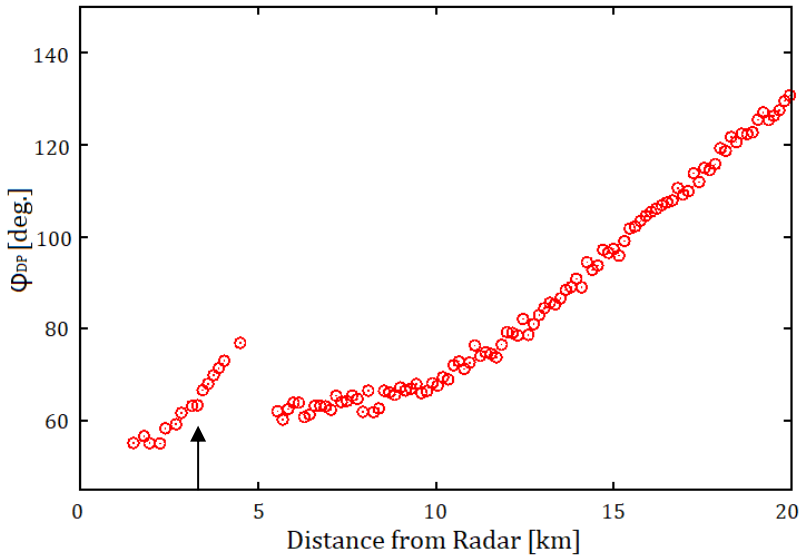

Figure 7 Range distribution of φDP observed by Asakura radar at PPI scan of 5.0 deg. in elevation angle. at 15: 28 JST, Sep. 17, 201. An arrow shows the location of Kochi city hall.

Table 3 shows the result of verification of QPE for each distance from radar. Except Monobe radar, the tendency of underestimation became remarkable at farer regions from radar. We considered that it was caused by two reasons. The first is the effect of altitude estimating *Rr*. The observation height becomes higher with the distance from radars. When cloud yielding rainfall developed lower altitude like as warm rain case, the radar beam passing in high altitude may return just weak echoes. Aki radar showed strongly this trend because low elevation beams blocked by mountains near Aki radar site and *Rr* farer than 10 km was estimated from the PPI scan at higher elevation angles. The altitude of about 3 km. Second is the azimuth resolution of radar beam. Because our radars are compact, beam widths are large as shown in Table 1. Then, the azimuth and height

Table 3 Regression and correlation coefficient at each distance

Distance from radar [km]	Asakura		Monobe		Aki	
	a	*r*	*a*	*r*	*a*	*r*
0-10	1.07	0.88	1.01	0.81	0.95	0.87
10-20	0.88	0.84	1.04	0.79	1.31	0.78
20-30	0.81	0.75	0.99	0.7	0.78	0.56
30-	0.72	0.68	-	-	-	-

resolution becomes worse with the distance from radars. At 20 km distance from a radar, the azimuth resolution of Asakura radar is approximately 670 and those of Monobe and Aki radar are 940 m.

7 Conclusion

We evaluated the accuracy of Quantitative Precipitation Estimation obtained from Asakura, Monobe, and Aki radars by comparing with rainfall intensity obtained by rain gauges. Asakura and Aki radars slightly underestimated rainfall intensity and Monobe radar showed good performance. The correlation between the radars and rain gauges were almost 0.8, which shows that QPE by our radars were accurate. On the other hand, radar underestimated rainfall at the regions far from radars. But we expect that this problem will be solved by merging radar data in our radar network.

We will make quality control of each radar data more to improve the accuracy of QPE and investigate the reason of abnormal reflectivity at some observation points as future works.

Acknowledgements

This research and development work was supported by the MIC/SCOPE 165009001. A part of rain gauge data was provided from Japan Meteorological Agency and Railway Technical Research Institute.

References

Aoyagi, J. ,1983: A study on the MTI weather radar system for rejecting ground clutter, Papers in Meteorology and Geophysics, Vol. 33, No. 4, pp. 187-243.

Cressman, G.P., 1959 : An operational objective analysis system, Monthly Weather Review, 87, pp. 367-374.

Fujiwara, M., 1965: Raindrop-size distribution from individual storms, Journal of Atmospheric Sciences, 22, 5, pp.585-591.

Hubbert, J. and Bringi, V.N., 1995: An iterative filtering technique for the analysis of copolar differential phase and dual-frequency radar measurements, J. Atmos. Ocean. Technol., 12, pp.643-648.

Maesaka, T., Maki,M., Iwanami, K., Tsuchiya, S., Kieda,K., and Hoshi, A. 2011: Operational rainfall estimation by X-band MP radar network in MLIT, Japan, Proc. of 35th Conf. on Radar Meteor, 142.

Maki, M., Part, S.-G., and Bringi, V.N., 2005: Effect of variations in rain drop size distributions on rain rate estimations of 3 cm wavelength polarimetric radar, Journal of the Meteorological Society of Japan, Vol. 83, No. 5, pp.871-893

Park, S.G., M. Maki, K. Iwanami, V. N. Bringi, and V. Chandrasekar, 2005: Correction of radar reflectivity and differential reflectivity for rain attenuation at X band. Part II: evaluation and application, J. Atmos. Ocean. Technol., 22, pp. 1633-1655.